



A new family of octanuclear Mn complexes with a rod-like topology

Eleni E. Moushi^a, Theocharis C. Stamatatos^b, Vassilios Nastopoulos^c, George Christou^b, Anastasios J. Tasiopoulos^{a,*}

^a Department of Chemistry, University of Cyprus, 1678 Nicosia, Cyprus

^b Department of Chemistry, University of Florida, Gainesville, FL 32611-7200, USA

^c Department of Chemistry, University of Patras, 26500 Patras, Greece

ARTICLE INFO

Article history:

Available online 13 May 2009

Dedicated to Dr. Aris Terzis in recognition of his great help for the advancement of inorganic chemistry in Greece through single-crystal X-ray crystallography.

Keywords:

Mn clusters

1,3-Propanediol

Crystal structures

Magnetic properties

ABSTRACT

Three new octanuclear compounds were prepared from reactions of $[Mn(O_2CR)_2] \cdot 2H_2O$ ($R = Et$ or Ph) with the diols 1,3-propanediol (pdH_2) or 2-methyl-1,3-propanediol ($mpdH_2$) in the presence of NaN_3 . All three compounds $[Mn_8(N_3)_4(O_2CR)_6(L)_4(py)_6]$ ($L = pd^{2-}$, $R = Et$ **1**; $L = mpd^{2-}$, $R = Et$ **2**; $L = pd^{2-}$, $R = Ph$ **3**) ($py = pyridine$) possess a novel near-planar, rod-like topology. DC and AC magnetic susceptibility studies in the 2–300 K range for complexes **1** and **2** revealed the presence of dominant antiferromagnetic exchange interactions, leading to diamagnetic ground spin states.

© 2009 Elsevier Ltd. All rights reserved.

1. Introduction

The synthesis of polynuclear Mn clusters has attracted significant interest since such compounds have potential applications in a number of areas including bioinorganic chemistry and materials science. In the former area, it is known that polynuclear Mn clusters are present in the active sites of metalloenzymes, the most important of which is the Mn_4 complex that is present in the active site of photosystem II (PS II) and is responsible for the light-driven oxidation of water to molecular O_2 [1]. Thus, intense synthetic efforts have been concentrated towards the preparation of Mn clusters that model the structure, spectroscopic properties and/or function of the Mn_4 cluster of PS II [1b]. The interest from the materials science point of view was stimulated by the discovery that $[Mn_{12}O_{12}(O_2CMe)_{16}(H_2O)_4]$ can function as single-domain magnetic particle at low temperatures, displaying magnetization hysteresis and quantum tunneling of the magnetization (QTM) [2]. Molecules that display such behavior have been termed ‘single-molecule magnets’ (SMMs) and derive their properties from a combination of a large ground state spin (S) value with a large and negative (easy-axis type) magnetoanisotropy [2]. Although a number of SMMs have been prepared with a variety of paramagnetic metal ions, manganese chemistry is still the most fruitful

source of SMMs since polynuclear manganese complexes often combine large, and sometimes abnormally large, ground spin states (currently up to 83/2) [3] with large negative D values [2,4–9].

One of the most successful synthetic approaches to new high nuclearity Mn clusters involves the use of chelating ligands containing alkoxide functions, since these are good bridging groups, and thus, favor the formation of polynuclear products [4]. With this in mind, we have been exploring the use of 1,3-propanediol (pdH_2) and 2-methyl-1,3-propanediol ($mpdH_2$) in Mn carboxylate chemistry. These studies have resulted in a number of new polynuclear clusters, some of which display large nuclearities, new structural topologies and interesting magnetic properties [8–11]. A recent extension of these investigations included the use of the N_3^- anion together with the (m) pdH_2 ligand, in Mn carboxylate chemistry. Our aim was the preparation of polynuclear compounds with large spin ground state values, since the N_3^- ligand results in ferromagnetic exchange interactions when it bridges metal ions in the 1,1 (end-on) fashion, for a wide range of $M-N-M$ angles [12]. The initial result of these investigations was a family of compounds that contain the $[Mn_1^{III}Mn_6^{II}(\mu_4-O)_8(\mu_3-L)_4]^{25+}$ ($L = N_3^-$ or OCN^-) octahedral unit appearing in a discrete cluster and in 1- and 2-D coordination polymers [9,10]. The discrete Mn_{17} cluster was found to have an $S_T = 37$ ground state, the second largest known to date, and to display SMM behavior [9].

We herein report further investigations on the use of the combination of (m) pdH_2 and N_3^- ligands in Mn carboxylate chemistry,

* Corresponding author. Tel.: +357 22892765; fax: +357 22892801.
E-mail address: atasio@ucy.ac.cy (A.J. Tasiopoulos).

which have produced a new family of octanuclear complexes $[\text{Mn}_8(\text{N}_3)_4(\text{O}_2\text{CR})_6(\text{L})_4(\text{py})_6]$ ($\text{L} = \text{pd}^{2-}$, $\text{R} = \text{Et}$ **1**; $\text{L} = \text{mpd}^{2-}$, $\text{R} = \text{Et}$ **2**; $\text{L} = \text{pd}^{2-}$, $\text{R} = \text{Ph}$ **3**) with a near-planar, rod-like topology. The magnetic properties of compounds **1** and **2** were studied by dc and ac magnetic susceptibility measurements, which revealed that both compounds have a diamagnetic spin ground state.

2. Experimental

2.1. General and physical measurements

All manipulations were performed under aerobic conditions using materials (reagent grade) and solvents as received; water was distilled in-house. *Warning: Although no such behavior was observed during the present work, azide salts are potentially explosive; such compounds should be used in small quantities, and treated with utmost care at all times.* $\text{Mn}(\text{O}_2\text{CEt})_2 \cdot 2\text{H}_2\text{O}$ [13], $\text{Mn}(\text{O}_2\text{CPh})_2 \cdot 2\text{H}_2\text{O}$ [14] were synthesized according to published methods. Elemental analyses (C, H, N) were performed by the in-house facilities of the University of Florida, Chemistry Department.

2.2. Compound preparation

2.2.1. $[\text{Mn}_8(\text{N}_3)_4(\text{O}_2\text{CEt})_6(\text{pd})_4(\text{py})_6]$ (**1**)

To a solution of $[\text{Mn}(\text{O}_2\text{CEt})_2] \cdot 2\text{H}_2\text{O}$ (0.131 g, 0.553 mmol) in a 10:2 ml mixture of MeCN/py was added pdH₂ (0.20 ml, 2.77 mmol) and NaN₃ (0.036 g, 0.55 mmol). The resulting yellowish-brown slurry was then left under magnetic stirring for 10 min. Then, it was filtered off, and the filtrate was left undisturbed at room temperature. After a few days X-ray quality crystals appeared and were collected by filtration, washed with MeCN and dried in vacuum. The yield was 36%. Elemental analysis: *Anal.* calc. for C₆₀H₈₄O₂₀N₁₈Mn₈ (**1**): C 39.66, H 4.66, N 13.88. Found: C 39.82, H 4.64, N 13.78%. Selected IR data (KBr): $\nu \sim = 3441\text{cm}^{-1}$, br, 2980w, 2937w, 2856w, 2073s, 1566s, 1427s, 1300w, 1087s, 1051s, 941w, 817w, 596w, 523w.

2.2.2. $[\text{Mn}_8(\text{N}_3)_4(\text{O}_2\text{CEt})_6(\text{mpd})_4(\text{py})_6]$ (**2**)

To a solution of $[\text{Mn}(\text{O}_2\text{CEt})_2] \cdot 2\text{H}_2\text{O}$ (0.107 g, 0.450 mmol) in a 10:2 ml mixture of MeCN/py was added mpdH₂ (0.20 mL, 2.25 mmol) and NaN₃ (0.029 g, 0.45 mmol). The resulting yellowish - brown slurry was left under magnetic stirring for 15 min. Then, it was filtered off, and the filtrate was left undisturbed at room temperature. After a few days, X-ray quality crystals appeared and were collected by filtration, washed with MeCN and dried in vacuum. The yield was 34%. Elemental analysis: *Anal.* calc. for C₆₄H₉₂O₂₀N₁₈Mn₈ (**2**): C 41.04, H 4.95, N 13.46. Found: C 41.27, H 5.03, N 13.31%. Selected IR data (KBr): $\nu \sim = 3412\text{cm}^{-1}$, br, 2979w, 2937w, 2877w, 2862w, 2077s, 1570s, 1429s, 1300w, 1110m, 1042m, 1042m, 951w, 817w, 590m, 537w.

2.2.3. $[\text{Mn}_8(\text{N}_3)_4(\text{O}_2\text{CPh})_6(\text{pd})_4(\text{py})_6]$ (**3**)

To a solution of $[\text{Mn}(\text{O}_2\text{CPh})_2] \cdot 2\text{H}_2\text{O}$ (0.184 g, 0.552 mmol) in a 10:2 ml mixture of Me₂CO/py was added pdH₂ (0.20 mL, 2.77 mmol) and NaN₃ (0.036 g, 0.55 mmol). The resulting yellowish-brown slurry was left under magnetic stirring for 15 min. Then, it was filtered off, and the filtrate was left undisturbed at room temperature. After a few weeks X-ray quality crystals appeared and were collected by filtration, washed with Me₂CO and dried in vacuum. The yield was 23%. Elemental analysis: *Anal.* calc. for C₈₄H₈₄O₂₀N₁₈Mn₈ (**3**): C 47.93, H 4.02, N 11.98. Found: C 47.78, H 4.12, N 12.06%. Selected IR data (KBr): $\nu \sim = 3453\text{cm}^{-1}$, br, 2942w, 2856w, 2070s, 1601s, 1558s, 1445w, 1399s, 1088m, 1052m, 944w, 817w, 723w, 593w.

Table 1
Crystallographic data for complexes **1** and **2**.

Parameter	1	2
Formula	C ₆₀ H ₈₄ Mn ₈ N ₁₈ O ₂₀	C ₆₄ H ₉₂ Mn ₈ N ₁₈ O ₂₀
Formula weight	1816.97	1873.08
Crystal system	triclinic	triclinic
Space group	P \bar{T}	P \bar{T}
<i>Unit cell dimensions</i>		
<i>a</i> (Å)	11.887(2)	11.710(1)
<i>b</i> (Å)	18.562(3)	11.963(1)
<i>c</i> (Å)	19.279(3)	16.307(2)
<i>a</i> (°)	75.43(2)	74.522(6)
<i>b</i> (°)	76.25(2)	88.365(6)
<i>c</i> (°)	72.05(2)	78.679(5)
<i>V</i> (Å ³)	3857(1)	2158.1(3)
<i>Z</i>	2	1
ρ_{calc} (Mg m ⁻³)	1.564	1.441
Radiation, λ (Å)	Mo K α , 0.71073	Mo K α , 0.71073
Temperature (K)	100(2)	100(2)
μ (mm ⁻¹)	1.343	1.203
Data collected/unique (R_{int})	54646/14354(0.0506)	38159/10853(0.0297)
Data with $I > 2\sigma(I)$	7368	6698
R_1 ($I > 2\sigma(I)$) ^a	0.0324	0.0366
wR ₂ ($I > 2\sigma(I)$) ^b	0.0592	0.0952

^a $R_1 = \sum(|F_0| - |F_c|) / \sum(|F_0|)$.

^b $wR_2 = \{\sum[w(F_o^2 - F_c^2)^2] / \sum[w(F_o^2)^2]\}^{1/2}$.

2.3. Single-crystal X-ray crystallography

Crystals of **1**, **2** and **3** in Paratone-N oil were mounted on glass fibers. Diffraction measurements were made on an Oxford Diffraction CCD instrument using graphite-monochromated Mo radiation. Complete crystal data and parameters for data collection and processing are reported in Table 1. Unit cell dimensions were determined and refined by using 12620 ($3.1^\circ \leq \theta \leq 30.6^\circ$) and 15442 ($3.1^\circ \leq \theta \leq 30.4^\circ$) reflections for **1** and **2**, respectively. Empirical absorption corrections (multi-scan based on symmetry-related measurements) were applied using CRYSTALIS RED software [15]. Data for **3** were of insufficient quality to allow full structure analysis but were suitable for the atom connectivity, and chemical formula to be confirmed; crystal data of **3** thus are not included in Table 1.

The structures were solved by direct methods using SIR92 [16a] and refined by full-matrix least-squares techniques on F^2 using SHELXL97 [16b]. Programs used: CRYSTALIS CCD [15] for data collection, CRYSTALIS RED [15] for cell refinement and data reduction, and DIAMOND [17a] and MERCURY [17b] for molecular graphics. All non-hydrogen atoms of the two structures were refined anisotropically. The hydrogen atoms attached to carbon atoms of the ligands of compounds **1** and **2** were positioned geometrically (riding model).

2.4. Other measurements

IR spectra (4000–400 cm⁻¹) were recorded at the University of Cyprus, using a Shimadzu Prestige – 21 spectrometer with samples prepared as KBr pellets. Variable-temperature dc and ac magnetic susceptibility data were collected at the University of Florida using a Quantum Design MPMS-XL SQUID susceptometer equipped with a 7 T magnet. The sample was embedded in solid eicosane to prevent torquing. Diamagnetic corrections to the observed susceptibilities were applied using Pascal's constants.

3. Results and discussion

3.1. Synthesis

Recently, we have been exploring the use of a combination of N₃⁻ and (m)pdH₂ ligands in Mn carboxylate chemistry. The initial

results of this investigation were the 1-D coordination polymers $[\text{Mn}_{17}(\mu_4\text{-O})_8(\text{N}_3)_5(\text{O}_2\text{CMe})_4(\text{L})_{10}(\text{py})_6]_\infty$ ($\text{L} = \text{pd}^{2-}$, **4** or mpd^{2-} , **5**), consisting of Mn_{17} octahedral units [9,10]. These compounds were isolated from the reaction of $[\text{Mn}(\text{O}_2\text{CMe})_2]\cdot 4\text{H}_2\text{O}$, pdH_2 (or mpdH_2) and NaN_3 in a 1:5:1 ratio in MeCN/py (py = pyridine). A number of modifications were performed to this reaction system, some of which resulted in a discrete Mn_{17} cluster and also in a 2-D coordination polymer consisting of the same Mn_{17} octahedral unit discussed above [9] and some others resulted in microcrystalline precipitates that we were unable to further characterize. However, the reactions which involved the use of different $[\text{Mn}(\text{O}_2\text{CR})_2]$ starting materials resulted in the isolation of three new octanuclear compounds with a rod-like topology (**1–3**). Thus, the reaction of $[\text{Mn}(\text{O}_2\text{CEt})_2]\cdot 2\text{H}_2\text{O}$ with pdH_2 and NaN_3 in a 1:5:1 ratio in MeCN/py (10/2 ml) resulted in the formation of yellowish-brown crystals of **1** in 36% yield. Analogous reactions, using mpdH_2 instead of pdH_2 , and $[\text{Mn}(\text{O}_2\text{CPH})_2]\cdot 2\text{H}_2\text{O}$ as a starting material instead of $[\text{Mn}(\text{O}_2\text{CEt})_2]\cdot 2\text{H}_2\text{O}$ were also performed, resulting in the forma-

tion of yellowish-brown crystals of complexes **2** and **3** in 34 and 23% yields, respectively. Note that crystals of **3** were isolated only when the reaction took place in an $\text{Me}_2\text{CO}/\text{py}$ solvent system. Although all the reactions took place in organic solvents (MeCN/py , $\text{Me}_2\text{CO}/\text{py}$) where NaN_3 is nearly insoluble, we should not forget that the solvents, which were used as received, contain small amounts of water and thus NaN_3 is slightly soluble in these solvent systems. The NaN_3 that comes in the solution reacts rapidly, more NaN_3 is then dissolved and the color of the reaction mixture changes to darker yellowish-brown as the reaction proceeds.

Compounds **2** and **3** are similar to **1** since they all possess the same structural core and differ from **1** mainly in the propanediol (mpd^{2-} instead of pd^{2-} in **2**) or the carboxylate ($-\text{O}_2\text{CPh}$ instead of $-\text{O}_2\text{CEt}$ in **3**) ligand they contain. In all those reactions, the oxidation state of the starting material is 2+, whereas the average oxidation state of the final products is higher, i.e. 2.25+ although no oxidant was added in the reaction mixture; we believe that the atmospheric O_2 is responsible for this oxidation which is facilitated

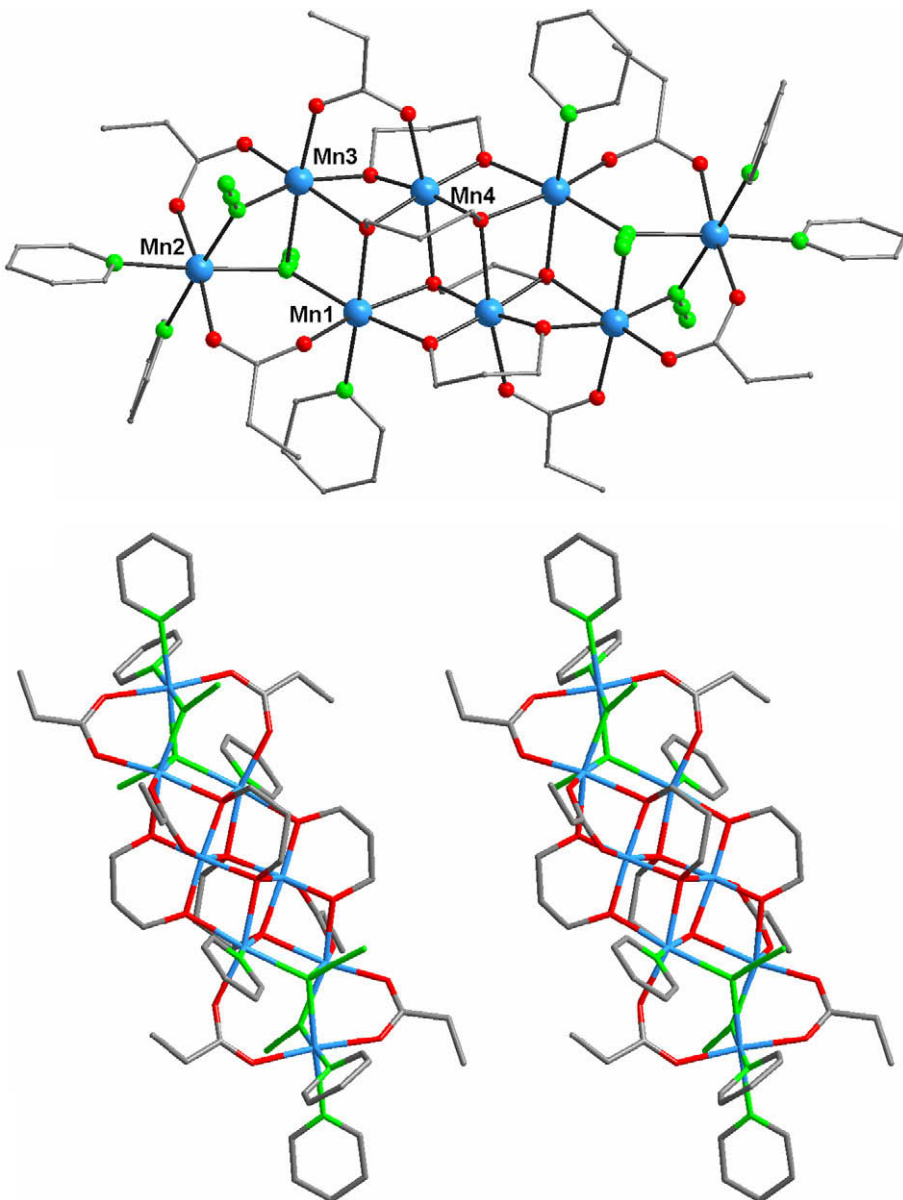
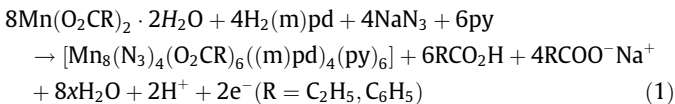


Fig. 1. Molecular structure (top) and stereoview (bottom) of complex **1**. Color code: Mn, blue; O, red; N, green; C, grey. (For interpretation of the references to colour in this figure legend, the reader is referred to the web version of this article.)

by the existence of a large excess of a base (pyridine) as it has also been observed in the past [18]. The formation of compounds **1–3** is summarized in Eq. (1).



The isolation of compounds **1–3** when $[\text{Mn}(\text{O}_2\text{CR})_2] \cdot 2\text{H}_2\text{O}$ ($\text{R} = \text{Et}$, or Ph) are used as starting materials does not imply that analogues of **4** and **5** with propionate and benzoate ligands respectively, are not formed as reaction co-products and vice versa. It is possible that the reaction solution in each case consists of a mixture of various species in equilibrium, which could include the analogues of **4** and **5**. However, since the identity of the product that is isolated from such reactions is determined by a number of factors such as relative solubility, lattice energies, crystallization kinetics, etc, it is reasonable that the use of different carboxylate ligands will result in the precipitation of different products.

3.2. Description of the structures

A partially labelled plot and a stereoview of **1** are shown in Fig. 1. A view of the structural core of **1–3** emphasizing its two butterfly units is shown in Fig. 2. Selected interatomic distances and BVS calculations data for compound **1** are listed in Tables 2 and 3, respectively. Since, the crystal structures of compounds **1–3** are strikingly similar, only the structure of **1** will be described in detail, and the other two structures will be compared to that of **1**. Complex **1** crystallizes in the triclinic space group $P\bar{1}$, with the asymmetric unit consisting of two halves of two octanuclear units of **1**. Bond-valence sum calculations (Table 3), charge considerations, and inspection of metric parameters revealed a mixed-valent complex containing six Mn^{II} and two Mn^{III} ions. The eight Mn ions of **1** are held together by bridging N_3^- and 1,3-propanediol ligands, resulting in a $[\text{Mn}_8^{\text{II}}\text{Mn}_2^{\text{III}}(\mu_3\text{-N}_3)_2(\mu\text{-N}_3)_2(\mu_3\text{-OR})_4(\mu\text{-OR})_4]^{6+}$ core (Fig. 2) with a near-planar, rod-like topology.

All eight Mn ions are in distorted octahedral geometries with the two Mn^{3+} ions displaying the expected Jahn-Teller elongations. The structure of **1** consists of two symmetry-related butterfly units, which are connected through RO⁻ groups of pd²⁻ ligands (Fig. 2). The four pd²⁻ ligands are fully deprotonated and two of them sit above and the other two below the plane of the core. Two of the pd²⁻ ligands bridge three Mn ions in a $\eta^2\text{:}\eta^2\text{:}\mu_3$ fashion, whereas the other two bridge five Mn ions in a $\eta^3\text{:}\eta^3\text{:}\mu_5$ fashion. The Mn^{2+} ions of each butterfly unit are held together by two end-on N_3^- ligands. One of the N_3^- group bridges three Mn^{2+} in a $\mu_3\text{-1,1,1}$ fashion, whereas the second N_3^- group bridges two Mn^{2+} ions in a $\mu_2\text{-1,1}$ fashion. The peripheral ligation of the compound is completed by six $\text{CH}_3\text{CH}_2\text{COO}^-$ ligands, and six terminal pyridine

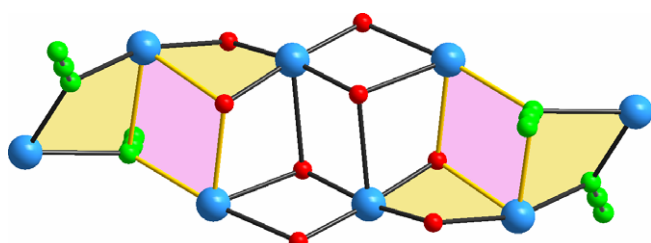


Fig. 2. The metal – oxygen–nitrogen core of **1**; the yellow lines connecting the Mn ions and the yellow and pink planes emphasise the two butterfly units. The color code is as in Fig. 1. (For interpretation of the references to colour in this figure legend, the reader is referred to the web version of this article.)

Table 2
Selected interatomic distances (Å) for complex **1**.

Bond Lengths			
Mn(1)–O(6)	2.110(2)	Mn(5)–O(12)	2.112(2)
Mn(1)–O(9)	2.190(2)	Mn(5)–O(19)	2.166(2)
Mn(1)–O(8)	2.260(2)	Mn(5)–N(13)	2.239(2)
Mn(1)–O(7)	2.269(2)	Mn(5)–O(18)	2.259(2)
Mn(1)–N(1)	2.316(2)	Mn(5)–O(17)	2.274(2)
Mn(1)–N(7)	2.328(2)	Mn(5)–N(10)	2.315(3)
Mn(2)–O(5)	2.150(2)	Mn(6)–O(11)	2.163(2)
Mn(2)–O(2)	2.175(2)	Mn(6)–O(15)	2.187(2)
Mn(2)–N(4)	2.228(2)	Mn(6)–N(16)	2.231(3)
Mn(2)–N(3)	2.291(2)	Mn(6)–N(12)	2.278(2)
Mn(2)–N(2)	2.329(3)	Mn(6)–N(11)	2.294(3)
Mn(2)–N(7)	2.355(2)	Mn(6)–N(13)	2.299(2)
Mn(3)–O(1)	2.118(2)	Mn(7)–O(16)	2.108(2)
Mn(3)–O(3)	2.127(2)	Mn(7)–O(14)	2.148(2)
Mn(3)–O(10)	2.166(2)	Mn(7)–O(20)	2.168(2)
Mn(3)–N(4)	2.215(2)	Mn(7)–N(16)	2.180(3)
Mn(3)–O(8)	2.285(2)	Mn(7)–O(17)	2.269(2)
Mn(3)–N(7)	2.390(2)	Mn(7)–N(13)	2.499(2)
Mn(4)–O(9)	1.890(2)	Mn(8)–O(19)	1.892(2)
Mn(4)–O(10)	1.897(2)	Mn(8)–O(20)	1.899(2)
Mn(4)–O(7)	1.948(2)	Mn(8)–O(18)	1.951(2)
Mn(4)–O(8)	1.970(2)	Mn(8)–O(17)	1.976(2)
Mn(4)–O(4)	2.223(2)	Mn(8)–O(13)	2.179(2)
Mn(4)–O(7)	2.460(2)	Mn(8)–O(18)	2.426(2)

Table 3
Bond-valence sums for the Mn atoms of **1**.^a

Atom	Complex 1		
	Mn^{II}	Mn^{III}	Mn^{IV}
Mn1	1.79	1.66	1.70
Mn2	1.88	1.78	1.76
Mn3	1.95	1.81	1.85
Mn4	3.04	2.78	2.92
Mn5	1.88	1.75	1.78
Mn6	1.93	1.83	1.81
Mn7	1.93	1.79	1.83
Mn8	3.07	2.81	2.95

^a The italicized value is the one closest to the charge for which it was calculated. The oxidation state of a particular atom can be taken as the nearest whole number to the italicized value.

groups. The six $\text{CH}_3\text{CH}_2\text{COO}^-$ ligands coordinate in their usual *syn, syn* μ_2 fashion. A close examination of the packing revealed that there are no intermolecular interactions between neighbouring Mn_8 units which are well separated since the shortest $\text{Mn}\cdots\text{Mn}$ distance between different Mn_8 units is relatively large (7.958 Å).

As it was mentioned above, the structures of compounds **2** and **3** are strikingly similar to this of **1** with the main differences between them being the diolate (mpd²⁻ in **2** instead of pd²⁻) or carboxylate (benzoate in **3** instead of propionate) ligands included in the compounds.

To our knowledge, the $[\text{Mn}_3^{\text{II}}\text{Mn}^{\text{III}}(\mu_3\text{-N}_3)(\mu\text{-N}_3)(\mu_3\text{-OR})(\mu\text{-OR})_2]^{4+}$ that is present in **1–3** is unknown in discrete form but would be particularly attractive since it is expected to have a large spin ground state because of the presence of the end - on N_3^- ligands. Complexes **1–3** are related to compounds $[\text{Mn}_8^{\text{II}}\text{O}_4(\text{O}_2\text{CCMe}_3)_{10}(\text{thme})_2(\text{py})_2]$ (**6**) [19] ($\text{H}_3\text{thme} = 1,1,1\text{-tris(hydroxymethyl)ethane}$) and $[\text{Mn}_4^{\text{II}}\text{Mn}_4^{\text{II}}(\text{O}_2\text{CCMe}_3)_2(\text{tmp})_2(\text{Htmp})_4\text{Br}_4(\text{H}_2\text{O})_2]$ (**7**) ($\text{H}_3\text{tmp} = 1,1,1\text{-tris(hydroxymethyl)propane}$) reported by Brechin and coworkers [18c] since they are all octanuclear Mn clusters with rod-like topologies. However, there are a number of significant differences between **1–3** and **6, 7** including: (i) the presence in **1–3** of end-on N_3^- ligands which lead in very different structural cores, (ii) the existence in **1–3** of fully deprotonated diols instead of triols, (iii) different oxidation states of the Mn ions, etc.

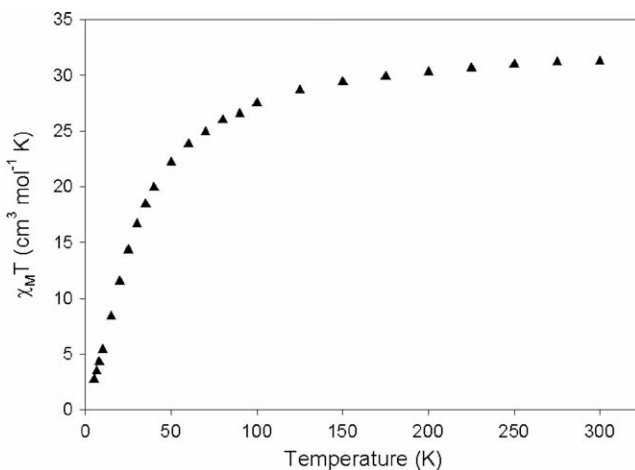


Fig. 3. Magnetic susceptibility data for **1**, shown as $\chi_M T$ vs T curves.

3.3. Magnetism

Variable-temperature, solid-state magnetic susceptibility measurements were performed on powdered polycrystalline samples of **1** and **2** in a 1kG (0.1T) field in the 5.0–300 K range. The obtained data for **1** and **2** are almost identical and thus only those for compound **1** are shown as a $\chi_M T$ vs T plot in Fig. 3. The $\chi_M T$ values at 300 K are 31.26 and 30.96 $\text{cm}^3 \text{mol}^{-1} \text{K}$ for **1** and **2** respectively. These values are slightly smaller than that expected for a cluster comprising six Mn^{II} and two Mn^{III} non-interacting ions ($32.25 \text{ cm}^3 \text{ mol}^{-1} \text{K}$ with $g = 2$). The $\chi_M T$ values gradually decrease with decreasing temperature to $22.15 \text{ cm}^3 \text{ mol}^{-1} \text{K}$ and $22.34 \text{ cm}^3 \text{ mol}^{-1} \text{K}$ at 50 K before dropping to $2.68 \text{ cm}^3 \text{ mol}^{-1} \text{K}$ and $2.52 \text{ cm}^3 \text{ mol}^{-1} \text{K}$ at 5.0 K. This behavior is indicative of the existence of dominant antiferromagnetic interactions between the metal centers, with the low temperature values suggesting a very small or zero ground spin state. In order to determine the ground state, magnetization data were collected in the temperature and magnetic field ranges 1.8–10.00 K and 0.1–7 T. Attempts were made to fit the resulting data using the program MAGNET [20], which assumes that only the ground state is populated at these temperatures and includes axial zero-field-splitting ($D\hat{S}_z^2$) and Zeeman interactions. However, it was not possible to obtain a satisfactory fit.

Reliable conclusions about the ground state S value, can nevertheless, be reached by using alternating current (ac) magnetic sus-

ceptibility measurements [5b,8,11]. The in-phase $\chi_M' T$ vs. T data for compound **1** are shown in Fig. 4. The $\chi_M' T$ signal for both compounds decreases linearly with decreasing temperature in the whole temperature range, and is clearly heading to $\chi_M' T$ values close to 0 at 0 K. This is consistent with the existence of antiferromagnetic interactions within the Mn ions of **1** and **2** and a diamagnetic ground spin state as was suggested on the basis of the dc magnetic susceptibility data. As expected for compounds with diamagnetic ground spin states, there are no out-of-phase ac signals down to 1.8 K.

An $S = 0$ ground state for compounds such as **1** and **2** with end-on N_3^- ligands, which are expected to mediate ferromagnetic interactions, is somewhat surprising. Since, the $[\text{Mn}_3^{\text{II}}\text{Mn}^{\text{III}}(\mu_3\text{-N}_3)(\mu\text{-N}_3)(\mu\text{-OR})(\mu\text{-OR})_2]^{4+}$ sub-unit does not exist in a discrete form in order to make relatively safe predictions about the sign and the magnitude of the various exchange interactions within **1** and **2**, it is quite difficult to rationalize the diamagnetic spin ground state. However, a rather simple and also reasonable rationalization of the $S = 0$ ground states of **1** and **2** is that whatever the ground state S of each of the two $[\text{Mn}_3^{\text{II}}\text{Mn}^{\text{III}}(\mu_3\text{-N}_3)(\mu\text{-N}_3)(\mu\text{-OR})(\mu\text{-OR})_2]^{4+}$ sub-units of the Mn_8 cluster might be, they are overall interacting antiferromagnetically with each other, and thus yield an $S = 0$ ground state for the complete molecule. Note, that compound **7**, which is the only other Mn_8 cluster with a planar rod-like topology, also has an $S = 0$ ground state [18c].

4. Conclusions

The present work is an extension of our investigations on the use of a combination of pdH₂ or mpdH₂ and N₃⁻ ligands in Mn carboxylate chemistry [9,10]. This study has produced a new family of octanuclear manganese complexes with a near-planar, rod-like topology which appears for first time in Mn-(m)pdH₂ chemistry. In addition, compounds **1–3** are the first that combine the rod-like topology with the presence of end-on N₃⁻ ligands and thus their $[\text{Mn}_6^{\text{II}}\text{Mn}_2^{\text{III}}(\mu_3\text{-N}_3)_2(\mu\text{-N}_3)_2(\mu_3\text{-OR})_4(\mu\text{-OR})_4]^{6+}$ structural core is unprecedented in Mn cluster chemistry. Magnetic susceptibility studies revealed the existence of antiferromagnetic exchange interactions within the Mn₈ unit that result in a diamagnetic ground state. Finally, it is clear that the Mn-(m)pdH₂ chemistry is proving a rich source of new polynuclear compounds. Further studies are thus in progress, which are expected to result in a number of new Mn clusters with a variety of structural topologies in the near future.

Supplementary data

CCDC 724079 and 724080 contains the supplementary crystallographic data for this paper. These data can be obtained free of charge via <http://www.ccdc.cam.ac.uk/conts/retrieving.html>, or from the Cambridge Crystallographic Data Centre, 12 Union Road, Cambridge CB2 1EZ, UK; fax: (+44) 1223-336-033; or e-mail: deposit@ccdc.cam.ac.uk.

Acknowledgements

This work was supported by the Cyprus Research Promotion Foundation (Grant: PENEK-ENISX/0505/18), and the USA National Science Foundation (CHE-0414555).

References

- [1] (a) J. Barber, Chem. Soc. Rev. 38 (2009) 185;
(b) S. Mukhopadhyay, S.K. Mandal, S. Bhaduri, W.H. Armstrong, Chem. Rev. 104 (2004) 3981.
- [2] (a) R. Sessoli, H.-L. Tsai, A.R. Schake, S. Wang, J.B. Vincent, K. Folting, D. Gatteschi, G. Christou, D.N. Hendrickson, J. Am. Chem. Soc. 115 (1993) 1804;

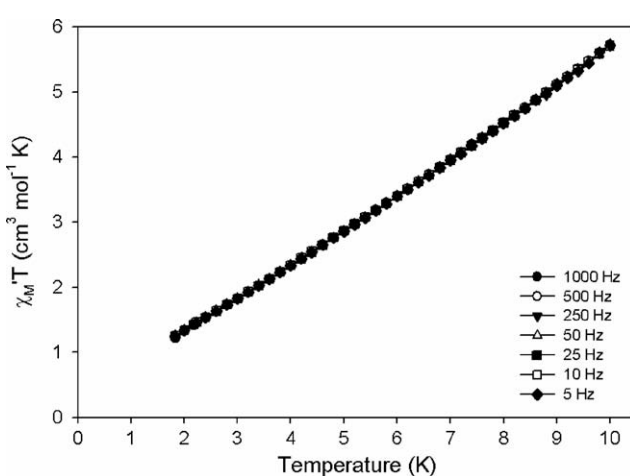


Fig. 4. Plot of the in-phase (χ_M') ac magnetic susceptibility as $\chi_M' T$ vs T for complex **1**, in a 3.5 Oe field oscillating at the indicated frequencies.

- (b) G. Christou, D. Gatteschi, D.N. Hendrickson, R. Sessoli, MRS Bull. 25 (2000) 66;
- (c) R. Sessoli, D. Gatteschi, A. Caneschi, M.A. Novak, Nature 365 (1993) 141.
- [3] (a) A.M. Ako, I.J. Hewitt, V. Mereacre, R. Clérac, W. Wernsdorfer, C.E. Anson, A.K. Powell, Angew. Chem., Int. Ed. 45 (2006) 4926;
- (b) O. Waldmann, A.M. Ako, H.U. Güdel, A.K. Powell, Inorg. Chem. 47 (2008) 3486.
- [4] (a) E.K. Brechin, Chem. Commun. (2005) 5141;
- (b) A.J. Tasiopoulos, S.P. Perlepes, Dalton Trans. (2008) 5537.
- [5] (a) A.J. Tasiopoulos, A. Vinslava, W. Wernsdorfer, K.A. Abboud, G. Christou, Angew. Chem., Int. Ed. 43 (2004) 2117;
- (b) A.J. Tasiopoulos, W. Wernsdorfer, K.A. Abboud, G. Christou, Inorg. Chem. 44 (2005) 6324;
- (c) C.J. Milios, C.P. Raptopoulou, A. Terzis, F. Lloret, R. Vicente, S.P. Perlepes, A. Escuer, Angew. Chem., Int. Ed. 43 (2004) 210;
- (d) C.M. Zaleski, E.C. Depperman, C. Dendrinou-Samara, M. Alexiou, J.W. Kampf, D.P. Kessissoglou, M.L. Kirk, V.L. Pecoraro, J. Am. Chem. Soc. 127 (2005) 12862;
- (e) C.M. Zaleski, E.C. Depperman, J.W. Kampf, M.L. Kirk, V.L. Pecoraro, Angew. Chem., Int. Ed. 43 (2004) 3912;
- (f) S. Maheswaran, G. Chastanet, S.J. Teat, T. Mallah, R. Sessoli, W. Wernsdorfer, R.E.P. Winpenny, Angew. Chem., Int. Ed. 44 (2005) 5044.
- [6] (a) R.T.W. Scott, S. Parsons, M. Murugesu, W. Wernsdorfer, G. Christou, E.K. Brechin, Angew. Chem., Int. Ed. 44 (2005) 6540;
- (b) S. Piligkos, G. Rajaraman, M. Soler, N. Kirchner, J. van Slageren, R. Bircher, S. Parsons, H.-U. Güdel, J. Kurtus, W. Wernsdorfer, G. Christou, E.K. Brechin, J. Am. Chem. Soc. 127 (2005) 5572;
- (c) D. Foguet-Albiol, T.A. O'Brien, W. Wernsdorfer, B. Moulton, M.J. Zaworotko, K.A. Abboud, G. Christou, Angew. Chem., Int. Ed. 44 (2005) 897;
- (d) C.J. Milios, M. Manoli, G. Rajaraman, A. Mishra, L.E. Budd, F. White, S. Parsons, W. Wernsdorfer, G. Christou, E.K. Brechin, Inorg. Chem. 45 (2006) 6782.
- [7] (a) C.J. Milios, A. Vinslava, W. Wernsdorfer, S. Moggach, S. Parsons, S.P. Perlepes, G. Christou, E.K. Brechin, J. Am. Chem. Soc. 129 (2007) 2754;
- (b) J.T. Brockman, T.C. Stamatatos, W. Wernsdorfer, K.A. Abboud, G. Christou, Inorg. Chem. 46 (2007) 9160;
- (c) T.C. Stamatatos, V. Nastopoulos, A.J. Tasiopoulos, E.E. Moushi, W. Wernsdorfer, G. Christou, S.P. Perlepes, Inorg. Chem. 47 (2008) 10081;
- (d) S.J. Shah, C.M. Ramsey, K.J. Heroux, A.G. DiPasquale, N.S. Dalal, A.L. Rheingold, E. del Barco, D.N. Hendrickson, Inorg. Chem. 47 (2008) 9569;
- (e) T.C. Stamatatos, S.J. Teat, W. Wernsdorfer, G. Christou, Angew. Chem., Int. Ed. 48 (2009) 521.
- [8] E.E. Moushi, T.C. Stamatatos, W. Wernsdorfer, V. Nastopoulos, G. Christou, A.J. Tasiopoulos, Angew. Chem., Int. Ed. 45 (2006) 7722.
- [9] E.E. Moushi, T.C. Stamatatos, W. Wernsdorfer, V. Nastopoulos, G. Christou, A.J. Tasiopoulos, Inorg. Chem. (2009), doi:10.1021/ic801795.
- [10] E.E. Moushi, T.C. Stamatatos, V. Nastopoulos, G. Christou, A.J. Tasiopoulos, Polyhedron (2009), doi:10.1016/j.poly.2008.12.023.
- [11] E.E. Moushi, C. Lampropoulos, W. Wernsdorfer, V. Nastopoulos, G. Christou, A.J. Tasiopoulos, Inorg. Chem. 46 (2007) 3795.
- [12] (a) A. Escuer, G. Aromí, Eur. J. Inorg. Chem. (2006) 4721;
- (b) E. Ruiz, J. Cano, S. Alvarez, P. Alemany, J. Am. Chem. Soc. 120 (1998) 11122;
- (c) T.C. Stamatatos, G. Christou, Inorg. Chem. 48 (2009) 3308.
- [13] T. Lis, Acta Crystallogr. Sect. B 33 (1977) 2964.
- [14] M.W. Wemple, H.-L. Tsai, S. Wang, J.P. Claude, W.E. Streib, J.C. Huffman, D.N. Hendrickson, G. Christou, Inorg. Chem. 35 (1996) 6437.
- [15] Oxford Diffraction, CRYSTAL^{CCD} and CRYSTAL^{RED}, version p171.29.2, Oxford Diffraction Ltd, Abingdon, Oxford, England, 2006.
- [16] (a) A. Altomare, G. Cascarano, C. Giacovazzo, A. Guagliardi, M.C. Burla, G. Polidori, M. Camalli, J. Appl. Cryst. 27 (1994) 435;
- [b] G.M. Sheldrick, SHELXL97, University of Göttingen, Germany.
- [17] (a) K. Brandenburg, DIAMOND, Version 3.1d, Crystal Impact GbR, Bonn, Germany, 2006;
- (b) I.J. Bruno, J.C. Cole, P.R. Edgington, M. Kessler, C.F. Macrae, P. McCabe, J. Pearson, R. Taylor, Acta Crystallogr. Sect. B 58 (2002) 389.
- [18] (a) J. Yoo, A. Yamaguchi, M. Nakano, J. Krzystek, W.E. Streib, L.-C. Brunel, H. Ishimoto, G. Christou, D.N. Hendrickson, Inorg. Chem. 40 (2001) 4604;
- (b) R.P. John, K. Lee, B.J. Kim, B.J. Suh, H. Rhee, M.S. Lah, Inorg. Chem. 44 (2005) 7109;
- (c) M. Manoli, C.J. Milios, A. Mishra, G. Christou, E.K. Brechin, Polyhedron 26 (2007) 1923.
- [19] (a) E. K. Brechin, M. Soler, G. Christou, M. Helliwell, S.J. Teat, W. Wernsdorfer, Chem. Commun. (2003) 1276;
- (b) G. Rajaraman, M. Murugesu, E.C. Sañudo, M. Soler, W. Wernsdorfer, M. Helliwell, C. Muryn, J. Raftery, S.J. Teat, G. Christou, E.K. Brechin, J. Am. Chem. Soc. 126 (2004) 15445.
- [20] E.R. Davidson, MAGNET, Indiana University: Bloomington, IN.